Anal Bioanal Chem
DOI 10.1007/s00216-016-0042-7

PAPER IN FOREFRONT

# Peptide-based fluorescence biosensors for detection/measurement of nanoparticles

**Oluyemi Akinloye**[1,2] · **Ramanarayan Krishnamurthy**[3] · **David Wishart**[1,3] · **Greg G. Goss**[1,3]

Received: 6 April 2016 / Revised: 5 October 2016 / Accepted: 19 October 2016


**Abstract** The ability to detect and quantify nanoparticles is essential but there is currently no simple, sensitive, and rapid method for the detection of nanomaterials. We have developed a novel peptide-based fluorescence-based biosensor for detection and measurement of negatively charged engineered nanoparticles (ENPs). A peptide biosensor (seven lysine residues linked to a cysteine through a three glycine residue linker) with attached fluorescent probes—fluorescein-5-maleimide (F5M) and tetramethylrhodamine-5-maleimide (TMR5M)—was constructed. The fluorescent probes allow close monitoring of the molecular interaction of the labeled peptide with ENPs. The ENP–peptide interaction induces the formation of agglomerates that can be detected and measured by changes in the fluorescence intensities of the labeled peptides or/and by differential light scattering. The relative fluorescence intensities of F5M and TMR5M decreased in a concentration-dependent manner on interaction with various types of negatively charged ENPs (ZnO, $Fe_3O_4$, CeO, and single-walled carbon nanotubes). Differential light scattering measurements also showed increases in the hydrodynamic size of the complex. The interactions were not affected by the pH of aqueous media, where humic acid (1 μg/mL) quenched the fluorescence intensity of F5M by approximately 25 %, whereas that of TMR5M was completely quenched. Interference by humic acid at lower concentrations was less prevalent. This novel method is a simple, rapid, and inexpensive in situ assay that shows promise as a primary-level testing technique for detection of ENPs in environmental samples.

**Keywords** Nanoparticles · Peptide · Fluorescein · Biosensor · Detection · Measurement

**Electronic supplementary material** The online version of this article (doi:10.1007/s00216-016-0042-7) contains supplementary material, which is available to authorized users.

✉ Greg G. Goss
greg.goss@ualberta.ca

[1] Department of Biological Sciences, Faculty of Science, University of Alberta, Z512 Biological Sciences Building, 11455 Saskatchewan Drive, Edmonton, AB T6G 2E9, Canada

[2] Clinical Chemistry Unit, Department of Medical Laboratory Science, Faculty of Basic Medical Sciences, College of Medicine of the University of Lagos, PMB 12003, Idi-Araba, Lagos 100254, Nigeria

[3] National Institute for Nanotechnology, 11421 Saskatchewan Drive, Edmonton, AB T6G 2M9, Canada

## Introduction

Rapid advances in nanoscience have led to much greater use of engineered nanomaterials (ENMs) in a variety of applications, ranging from medicine [1] and materials science [2] to environmental remediation [3] and consumer products [4]. Because of their small size and unique surface properties, engineered nanoparticles (ENPs) have many desirable and useful properties. However, they can also interact with living cells in potentially undesirable manners [5–8]. The adverse effects of ENMs on living systems have highlighted the need to develop improved rapid detection and sensitive (detection range below 1 mg/L) systems to manage the risks associated with their accidental occupational exposure or environmental release. The current methods for measuring ENMs primarily use advanced microscopy techniques, including transmission electron microscopy, scanning electron microscopy, atomic force microscopy, scanning proton microscopy, and scanning near-field ultrasonic holography. More recently, single particle tracking analysis and field-flow fractionation coupled with inductively coupled plasma mass spectrometry has emerged

Published online: 30 November 2016

as another tool for identification of nanomaterials in aqueous samples [8]. However, all these methods require a substantial initial investment in equipment and operator training, have long times between sampling and readout (days to weeks), and require specific prior knowledge of the nanomaterial of interest. There is no system for the detection of ENMs in aqueous media that does not require significant investments of time and money. Attempts to develop simple spectrophotometric and fluorometric methods for the detection of the ENM themselves have not been successful, mainly because of the intrinsic peculiar characteristics and chemical nature of each nanomaterial. The lack of appropriate routine ENP detection and evaluation techniques remains one of the major challenges that may hinder acceleration of development and growth in the field of nanoscience.

Development of biosensors for detection of a specific analyte is widely recognized [9]. A biosensor is an analytical device that combines a recognition element with a transducer (detection element) for the detection of a biological analyte or chemical agents (target) [10–13]. The recognition process utilizes the affinity of the recognition element for the analyte, and the interaction information is transmitted as a measurable signal (electrical, optical, etc.) by the transducer [12]. Transducers include man-made electrochemical, optical, piezoelectric, thermal, and magnetic devices that can quantitatively monitor the biochemical reactions arising from the biosensing materials. Because of their high sensitivity and selectivity, biosensors offer outstanding promise in the development of an ultrasensitive assay for the detection of low concentrations of chemicals and substances such as ENPs in environmental media. Biosensors that rely on protein, especially antibodies, as the biomolecular recognition element are commonly used, and more complex protein-based affinity scaffolds are increasingly becoming popular. However, short unstructured peptides have several potential preferred advantages that can be exploited for biosensor development: (1) peptides are stable and resistant to harsh environments; (2) peptides can be synthesized easily and inexpensively; and (3) peptides can be more amenable than antibodies or scaffold protein to engineering at the molecular level [14–16]. Fluorescence labeling of the peptide, usually performed through either the side chain of a lysine residue or the side-chain sulfhydryl group of a cysteine residue [17], allows the transmission of interaction information as a measurable signal (fluorescence). Fluorescently labeled peptides are commonly used to make possible fluorescence microscopy and fluorescence imaging in cellular biology [18, 19] and medicine [20]. However, to the best of our knowledge, this is the first time that this technology has been applied to the detection of ENMs in environmental media. Our strategy was to design a fluorescently labeled, positively charged peptide that electrostatically interacts with negatively charged ENMs in solution. Hence we used this interaction as a primary-level test for rapid (minutes to hours) detection of the presence/absence and concentration of ENPs in environmental media, with secondary advanced testing (e.g., inductively coupled plasma mass spectrometry, field-flow fractionation coupled with inductively coupled plasma optical emission spectroscopy, electron microscopy) conducted only after detection.

Currently, two significant challenges are being posed to researchers and regulators with regard to nanomaterial toxicology. The first one is to understand the fate, behavior, bioavailability, and transformation of nanomaterials in the environment into which they are released. The second challenge is to devise simple and precise methods for detecting and measuring low concentrations of nanomaterials in environmental aquatic matrices and workplace environments. The current study has the potential of meeting the urgent need of developing rapid, efficient, and throughput testing strategies to detect or/and measure nanomaterial in environmental samples.

## Materials and experimental methods

### Nanoparticles and materials used in the study

Polymer-capped nano-sized $Fe_3O_4$, $CeO_2$, and ZnO were provided by Vive Crop Protection (Toronto, Canada). These are small (less than 10 nm) negatively charged metal oxide ENMs ($Fe_3O_4$, $CeO_2$, and ZnO) that were functionalized with a poly(acrylic acid) (PAA) polymer coating. The functionalization makes these ENMs highly dispersible and stable in suspension. The properties in solution are well characterized and have been reported previously [21]. The carboxy-functionalized 10–20-nm single-walled carbon nanotubes (SWCNTs) were manufactured by the National Research Council's Steacie Institute for Molecular Sciences [22]. These particles are well characterized, and the details have been published [21–27]. All other chemicals used in this study were of analytical grade and were obtained from Sigma (St Louis) unless otherwise noted.

### Design of engineered peptide and biosensors

Using standard peptide engineering techniques, we generated a simple polypeptide containing an N-terminally protected polylysine peptide with seven lysine residues linked to a cysteine through a three glycine residue spacer (Ac–KKKKKKKGGGC–OH). This molecule was synthesized according to our specifications by the Institute of Biomolecular Design, Edmonton, Canada. The theory behind the design involves use of the side chain amino group of polylysine residues, which confers a strong positive charge on the peptide. This peptide will then be electrostatically attracted to the negatively charged nanoparticles (ENPs). Similar custom-

designed negatively charged peptides can be designed to attract and interact with positively charged ENMs.

### Peptide labeling

Peptides were labeled with fluorescein-5-maleimide (F5M) or tetramethylrhodamine-5-maleimide (TMR5M) as fluorescent probes according to the manufacturer's instructions (Molecular Probes, USA) and with appropriate postlabeling cleaning steps. In summary, the concentrated fluorescent probe (50 mM dissolved in dimethyl sulfoxide) was added to the peptide solution (4.06 mM) in buffer containing 20.3 mM *N*-(2-hydroxyethyl)piperazine-*N*′-ethanesulfonic acid–KOH (pH 7.6), 50 mM KCl, and 2 mM tris(2-carboxyethyl)phosphine in a molar ratio of 5:1 (probe to peptide) (see Fig. S1 and Table S1). The mixture (125-μL final volume) was incubated for 2 h at room temperature with gentle shaking in the dark. The reactions were quenched by the addition of excess DDT (20 mM). The pure labeled peptide mixture was further purified by precipitation with acetone (1 mL) as described by Vives and Lebleu [17]. Briefly, 500 μL of cold acetone was added to the labeled peptide mixture. This mixture was vortexed for 15 s and allowed to stand for 30 min at -20 °C, followed by centrifugation at 30,000 *g* at 4 °C. The supernatant was carefully removed and the peptide pellet was suspended in 100 μL of tris(hydroxymethyl)aminomethane (Tris) buffer (100 mM, pH 6.8).

### Purification of labeled peptides by high-performance liquid chromatography

The synthesized fluorescein-labeled peptides were further purified with an Agilent 1100 high-performance liquid chromatography (HPLC) system with a semipreparative reverse-phase Gemini $C_{18}$ column (250 mm × 10 mm, 5 μm, 110 Å; Phenomenex, Torrance, CA, USA). The gradient elution system was as follows: solution A consisted of water–acetonitrile (98:2, v/v) with 0.1 % trifluoroacetic acid; solution B consisted of acetonitrile (100 %) with 0.1 % trifluoroacetic acid. The gradient elution program was as follows: 0 min, 0 % solution B; 10 min, 0 % solution B; 25 min, 25 % solution B; 40 min, 60 % solution B; 45 min, 80 % solution B; 50 min, 0 % solution B. The flow rate was 2 mL/min and the injection volume was 50 μL. Fluorescently labeled peptide fractions were manually collected and quantified by measurement of the absorbance at 220, 440, and 540 nm for peptide, F5M, and TMR5M respectively and also by measurement of the fluorescence of F5M ($\lambda_{ex}$ = 490 nm; $\lambda_{em}$ = 500–600 nm) and TMR5M ($\lambda_{ex}$ = 525 nm; $\lambda_{em}$ = 550–650 nm) with use of a fluorescence plate reader (see Figs. S2 and S3 for scans). The efficiency of labeling was calculated by consideration of the ratios of the peak area of unlabeled peptide to that of labeled peptide. Qualitative information on purified labeled peptides was obtained by liquid chromatography with mass-selective detection through atmospheric pressure ionization–electrospray in positive mode.

### Quantification of the thiol group

Quantification of thiol (SH) group was done with Ellmans's reagent. The bonded peptide SH group completely reacted with the maleimide dyes in reaction with the free peptide controls, which have intact SH groups. In summary, samples (labeled peptide in triplicate), controls (unlabeled peptide), and standard (acetylcysteine) were precipitated with double volume of trichloroacetic acid, and spun down at 1500 rpm for 15 min at room temperature. The supernatant was reacted with Ellman's reagent (Tris–HCl buffer, pH 8.9 and dithionitrobenzene) and measured at 412 nm. The serial dilution of the acetylcysteine standard was used to draw a standard curve (Fig. S2). The amount of SH group on our purified labeled peptide was extrapolated from the standard curve (Table S1). We demonstrated that the sulfhydryl thiol (R–SH) groups on our engineered peptides had completely reacted with available maleimide dyes, indicating successful binding of probes to peptide. We found that a fivefold molar excess of dye to peptide achieved 100 % saturation of the peptide R–SH reaction (Fig. S1).

### Labeled peptide–nanoparticle interaction

The nanoparticle stock solutions were prepared in deionized distilled water to 1 mg/mL and used in our reactions. Nanoparticle suspensions were sonicated for 30 s before preparation of stock solutions, and the solutions were vortexed for 30 s before the experiment. The concentration of labeled peptides after HPLC purification and the concentration of each biosensor in the products were calculated by use of the extinction coefficients of the peptide and fluorescent dyes as provided by the manufacturer (Invitrogen, USA). Appropriate volumes of nanoparticles and labeled peptide were reacted at room temperature. Briefly, 5.0 μL of probes was added to 15 μL of nanoparticles in 130 μL of buffer solution. The buffer solution was replaced with solution containing humic acid in those experiments examining interference of natural organic material (NOM).

### Preparation of humic acid solution

The natural organic medium was mimicked by humic acid solution according to the method of Hong and Elimelech [28]. Briefly, Suwannee River humic acid (Standard II, International Humic Substances Society) was used as a model NOM in natural aquatic systems. The humic acid stock solution was prepared by addition of 21.7 mg of dry humic acid

powder to 50 mL of deionized water (Barnstead), with the solution being stirred overnight. This solution was then filtered through a 0.22-μm cellulose acetate membrane (Corning, Corning, NY, USA) under a vacuum. The pH of the solution was raised from 3.6 (natural pH) to 8 by addition of NaOH, after which the solution was stored in the dark at 4 °C. Information on key properties of the Suwannee River humic acid has been provided by Hong and Elimelech [28].

## Results and discussion

### Production and purification of labeled peptides

The conceptual design of the study is illustrated in Fig. 1. We investigated whether engineered labeled peptides could be used for the detection of nanomaterials. It is known that in solution nanomaterials interact with proteins and peptides, which often provide bridges between nanomaterials, in a concentration-dependent manner [24, 29]. Additionally, protein and peptide are known to bind to nanomaterials, resulting in structural changes as defined by reduction in enzyme function [25, 26], aggregation, and precipitation [24, 25]. We designed a customized peptide with high positive charge at physiological pH by use of a seven-lysine amino acid sequence coupled to a terminal cysteine–glycine linker. The single cysteine residue ensures the end-labeling reaction with fluorescent maleimide dyes. We used two dyes—F5M and TMR5M—for sensitive light-based detection. These fluorescent probes have very high specificity in labeling SH groups of cysteine. The SH group was protected by dithiothreitol in the reaction mixture, which also facilitated the quenching of the unreacted fluorescent dyes, enabling us to purify only fluorescently labeled peptides. Figure 2 shows the chromatograms generated by HPLC with absorbance at 280 nm as an indicator of the purified peptide. Mass spectra of the labeled peptides are shown in the insets (Fig. 2), showing a peak at the appropriate $m/z$ ratio for each labeled peptide, demonstrating the ability to purify labeled peptides to more than 90 % purity.

### Nanoparticle–peptide interaction and agglomeration can be detected by dynamic light scattering, is stable, and occurs across a range of natural pH values

The reaction of positively charged polypeptide and negatively charged nanoparticles results in the formation of aggregates that are visible to the naked eye (Fig. 3, top left), and these reactions occur and are visible even at a nanoparticle concentration of 1 μg/mL. The reaction was analyzed by dynamic light scattering after 5 min or 30 min, and our results show that the complexes of peptides and ENP were stable and of consistent size over the 30-min test period (Fig. 3, bottom left). The ability to interact and form aggregates was independent of the materials tested in our testing regime, including both spherical and high aspect ratio materials (Fig. 3, top right). Alteration of the solution pH from 7 to 9 did not affect either the size or the polydispersity index (Fig. S4) of the agglomerates, whereas there was a trend for reduction in the size of the agglomerates at pH 5. The light scattering as measured by dynamic light scattering was concentration dependent (Fig. 3, bottom right), with higher concentrations of ENPs producing slightly larger aggregates after 5 min. According to the Derjaguin–Landau–Verwey–Overbeek theory [30], the increasing concentrations of ENPs will result in increasing bridging-mediated agglomeration, thereby explaining the larger aggregates seen in Fig 3 (bottom right). At lower pH, the negatively charged SWCNTs and PAA-coated materials used in these assays would experience some charge shielding, thereby explaining the overall reduced agglomeration potential at pH 5. Nevertheless, this interaction consistently occurs across a broad range of pH values (pH 5–9) that are representative of most natural waters as receiving waters for ENPs [31, 32].

### Concentration-dependent inhibition of fluorescence by ENPs

The potential for ENPs to interact with our custom-designed fluorescently labeled peptides is examined in Fig. 4. The potential for interfering autofluorescence from the nanoparticle itself was investigated as indicated by the first bar in each graph in Fig. 4. Autofluorescence was not detectable for every ENP (labeled and nanoparticle), thereby indicating there was no interference from the material itself in our assay. This control is essential for proper assessment of light-based assays involving ENPs [27].

We next examined whether the custom labeled peptides interact with our negatively charged ENPs in a dose-dependent manner by adding increasing amount of each ENP to a fixed concentration of custom labeled peptide. For F5M, early experiments (data not shown) revealed that the optimal peptide concentration was 4.95 μg/L, whereas for TMR5M, the optimal concentration was lower, 0.88 μg/L. Therefore, for each material, the fluorescence intensity of labeled peptide alone represented 100 % fluorescence intensity, and all data were normalized to 1.0 for each experiment. Addition of increasing concentration of PAA-coated $Fe_3O_4$ particles to 7.23 μM F5M-labeled peptide with a short mixing period immediately after addition resulted in a dose-dependent decrease in fluorescence intensity (Fig. 4a), with a more than 90 % reduction in fluorescence intensity at an ENP concentration of 100 μg/mL. This reduction occurred almost immediately on addition of the particles. All measurements were conducted within the first minute since we noticed agglomeration and precipitation occurring after 5 min (Fig. S5). The TMR5M-labeled peptide was a much more

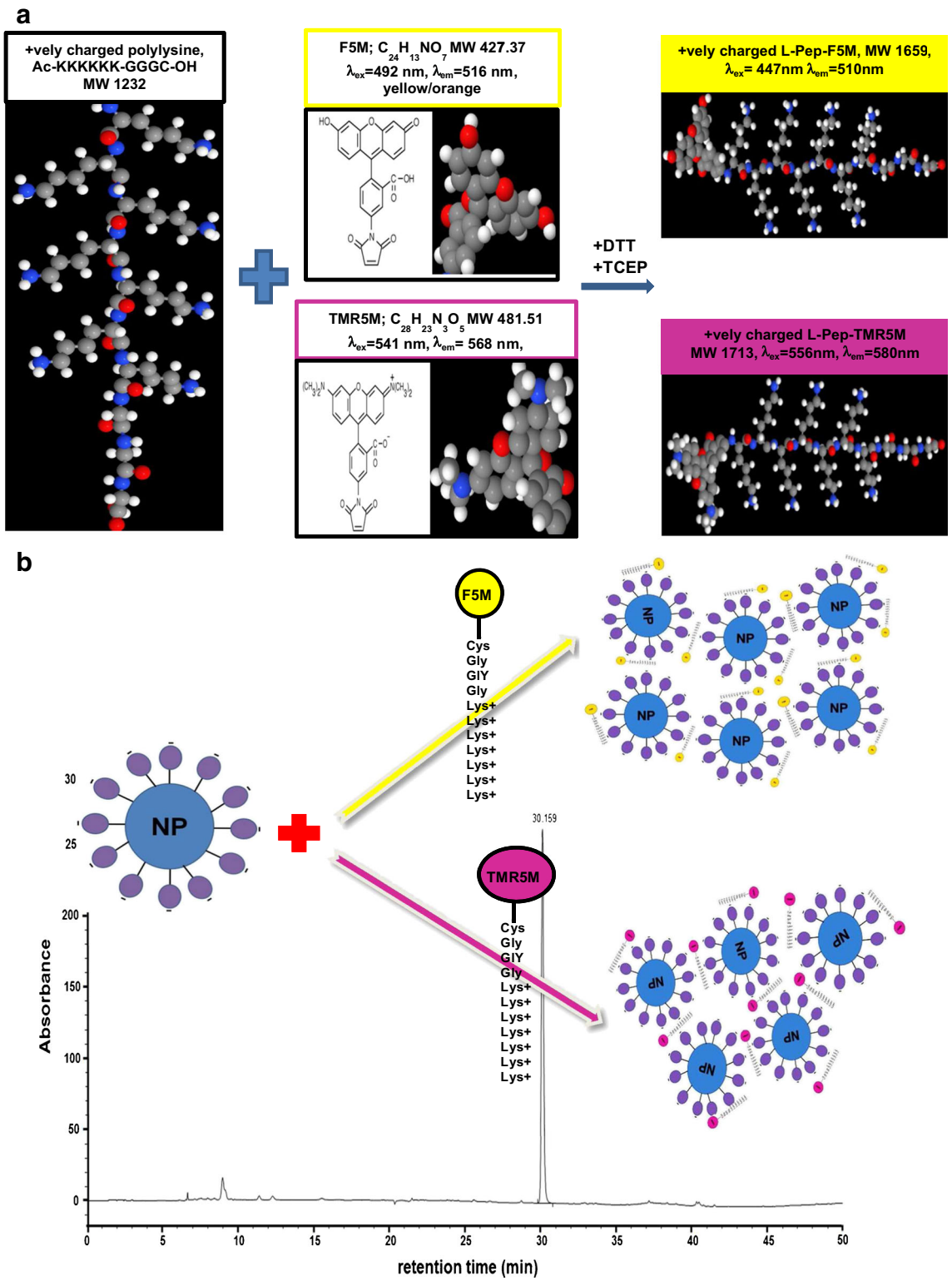


**Fig. 1** Summary of our fluorescein-labeled peptide detection of engineered nanomaterials (ENMs). The polypeptide developed for the biosensor is an N-terminally protected polylysine peptide with seven lysine residues linked to a cysteine through three glycine residues (Ac–KKKKKKKGGGC–OH). This molecule was synthesized according to our specifications by the Institute of Biomolecular Design, Edmonton, Canada. The side chain amino group of the polylysine residue confers a strong positive charge on the peptide. When added to a solution containing ENMs, the fluorescently labeled peptides will cause a general interaction with negatively charged ENMs, forming an aggregate. Attachment of fluorescein-5-maleimide (*F5M*) or tetramethylrhodamine-5-maleimide (*TMR5M*) to the polylysine peptide allows the use of these fluorescently labeled peptides to detect the present of ENMs quantitatively. The changes in relative fluorescein intensity of the aggregate can be detected by a throughput fluorescence microplate technique. *L-Pep* labeled peptide, *MW* molecular weight, *NP* nanoparticle

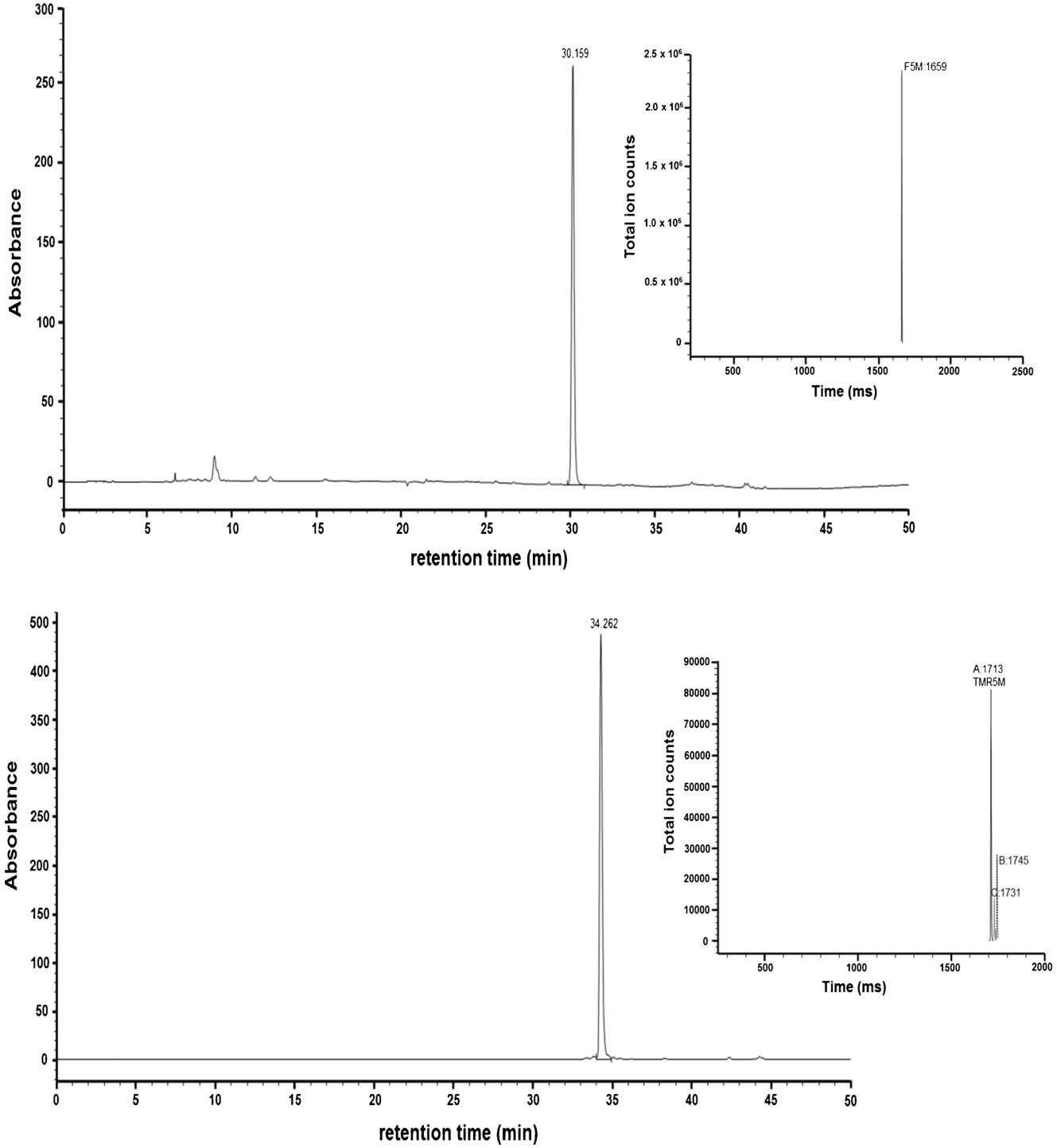


**Fig. 2** **a** High-performance liquid chromatography (HPLC) chromatogram of purified peptide labeled with F5M (L-Pep-F5M) with inserted mass spectrometry (MS) scan and **b** HPLC chromatogram of purified peptide labeled with TMR5M (L-Pep-TMR5M) with inserted MS scan. HPLC was performed with an Agilent 1100 HPLC system with a semipreparative Gemini $C_{18}$ column (250 mm × 10 mm, 5 μm, 110 Å; Phenomenex, Torrance, CA, USA) with use of a reverse-phase gradient elution system from 20 % solvent B to 80 % solvent B at a flow rate of 2 mL/min, with a stop time of 50 min and a post-stoppage time of 15 min (solvent A, 98 % $H_2O$, 2 % acetonitrile, 0.1 % trifluoroacetic acid; solvent B, 100 % acetonitrile and 0.1 % trifluoroacetic acid). Wavelength detection was performed at 220, 440, and 540 nm for peptide, F5M and TMR5M respectively. MS scans and qualitative information on purified L-Pep-F5M and L-Pep-TMR5M were obtained by liquid chromatography with mass-selective detection through atmospheric pressure ionization–electrospray in positive mode. Peptide molecular weight (MW) 1231.57 + F5M MW 427.37 = 1658.94 (1659) and peptide MW 1231.57 + TMR5M MW 481.51 = 1713.1 (1713)

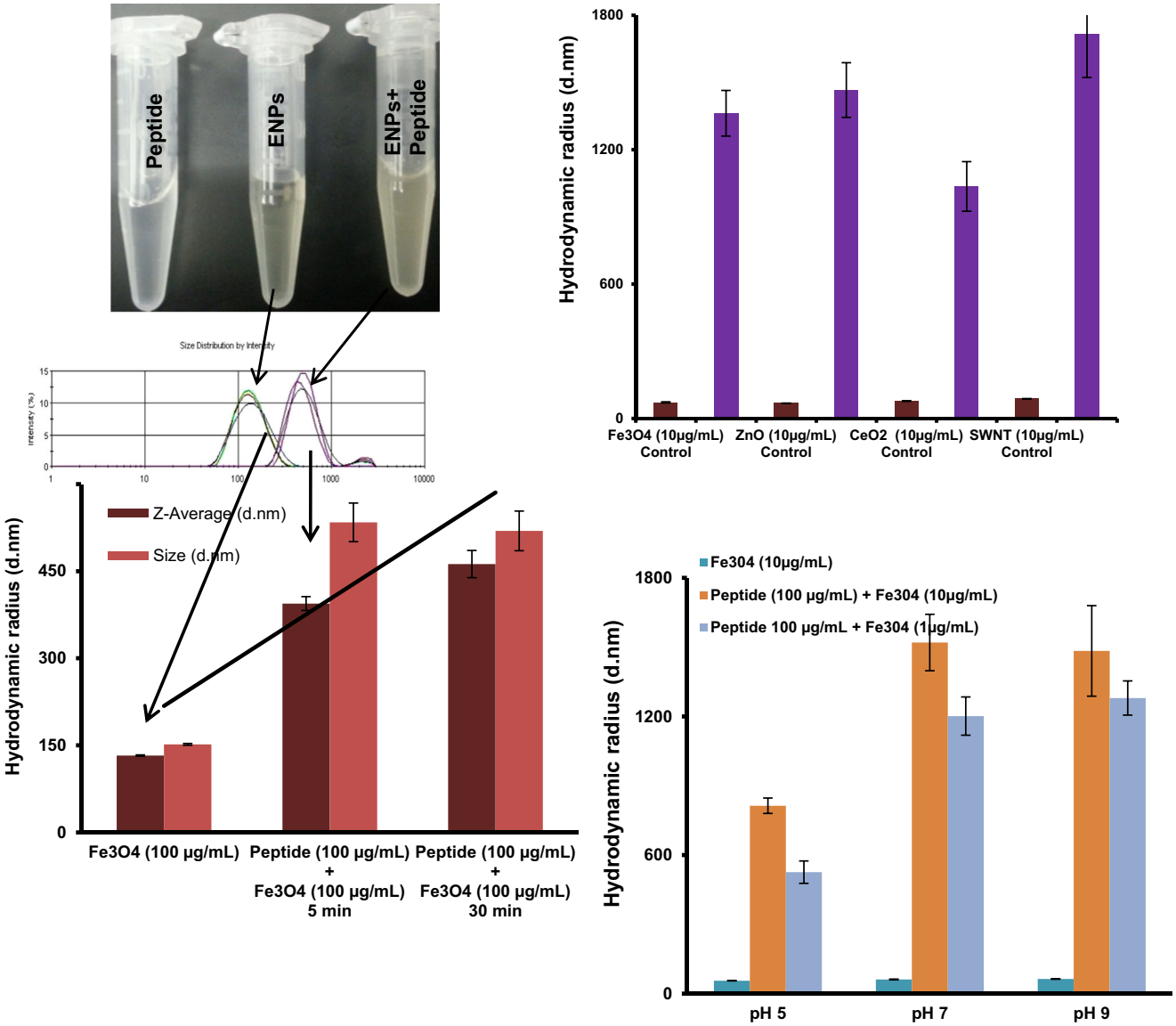


**Fig. 3** *Top left:* Visible light images showing turbidity formation of interaction between peptides at 100 µg/mL mixed with engineered nanopaticles (*ENPs*) at 100 µg/mL, with the reaction mixture incubated for 5 min at room temperature (pictures taken within 1 min). *Bottom left:* The dynamic light scattering readings for the reaction mixture incubated for 5 min and 30 min. *Top right*: The dynamic light scattering readings for similar reactions using different types of nanoparticles at 10 µg/L ($Fe_3O_4$, ZnO, $CeO_2$, single-walled carbon nanotubes). *Bottom right*: Reactions in medium of different pH. *SWNT* single-walled carbon nanotubes

sensitive indicator of ENP–particle interactions, with strong reductions in fluorescence intensity noted at an ENP concentration of 1 µg/mL despite the lower concentrations of peptide required for the assay (Figs. S6, S7, S8).

The PAA-coated ZnO or CeO or COO-functionalized SWCNTs produced results similar to those of the PAA-coated $Fe_3O_4$ material in Fig. 4a,, whereby increasing concentrations effected a reduction in the fluorescence intensity in a dose-dependent manner for both F5M-labeled and TMR5M-labeled peptides. In addition, TMR5M appeared to be a more sensitive indicator of the quantity of ENPs in the solution, providing significant reductions in fluorescence intensity at concentrations below 1 µg/mL and for COO-functionalized SWCNTs (Fig. 4 h); reductions in fluorescence intensity were noted even at 100 ng/mL.

We believe that the noted reduction in fluorescence intensity is likely not due to precipitation events as the measurements were taken immediately on mixing of ENPs and the labeled peptide and before agglomeration occurred. Instead, we suggest that the ENPs bind the labeled peptide and reduce the fluorescence intensity through a direct interaction between the labeled peptide and the ENPs. It is known that colloidal particles in solution bind peptides or other matter in solution, forming a corona of proteins, peptides, or other charged species as appropriate [33–35]. Moreover, it has been demonstrated that this binding results in alteration of the structure and

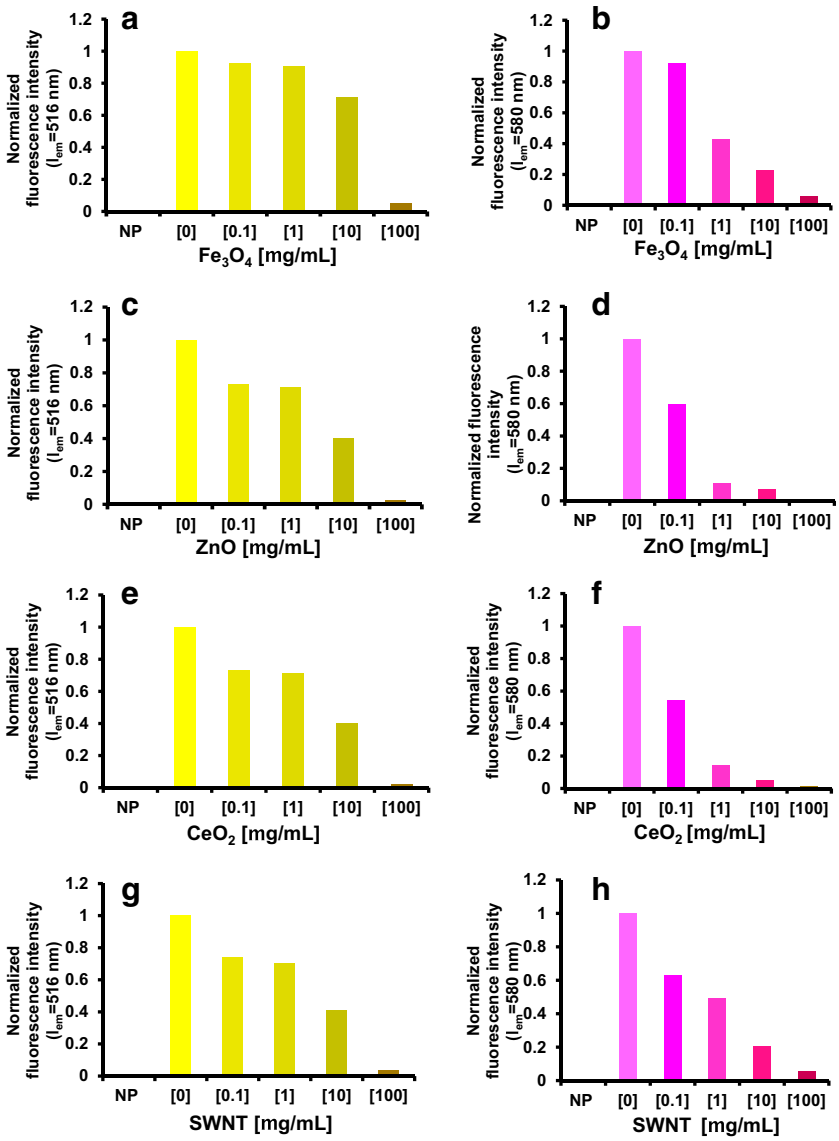


**Fig. 4** Concentration-dependent inhibition of fluorescence of fluorescein-5-maleimide-labeled peptide (P-F5M) and tetramethylrhodamine-5-maleimide-labeled peptide (P-TMR5M) after exposure to increasing concentrations (0.1, 1.0, 10, and 100 μg/mL) of different engineered nanomaterials ($Fe_3O_4$, CuO, CeO, and single-walled carbon nanotubes). The *y*-axis represents fluorescence intensity in arbitrary units (relative fluorescence units). P-F5M was excited at 447 nm and emitted at 522 nm, and P-TMR5M was excited at 566 nm and emitted at 580 nm. Nanomaterial-only controls were run at each concentration in the absence of the fluorescent peptides. *NP* nanoparticles, *SWNT* single-walled carbon nanotubes

function of other associated molecules [25, 26]. Binding of the peptide to the dye will alter the excitation and emission spectra of associated dyes [36], and this was seen in our preparation, where for F5M the excitation maximum of 492 nm shifted to 447 nm and the emission maximum shifted slightly from 516 to 518 nm. Similarly, for TMR5M, its excitation maximum shifted from 541 to 556 nm and its emission maximum shifted from 566 to 580 nm (data not shown). These shifts in the excitation and emission spectra can be attributed to stabilization of the fluorophore when it is bound to the peptide [36].

To examine whether this is the mechanism for the reduced fluorescence intensity, we performed a wavelength scan of the spectral characteristics of the dye with increasing concentration of ENPs. There was no associated spectral shift with increased ENP concentration for either F5M (Fig. 5a) or TMR5M (Fig. 5b), whereas a clear reduction in fluorescence intensity with increasing ENP concentration can be seen for PAA-coated $Fe_3O_4$ ENPs. Similar results were found for each of the other materials tested (data not shown). We believe that the additional stabilization of the dye associated with the interaction with the ENPs directly reduces the fluorescence intensity of the emitted light within the detection window. Importantly, we believe that these properties can be used in the development of a rapid and sensitive detection of the presence or absence of ENPs. One drawback of this detection method is that there is no ability to distinguish the identity of different materials or to distinguish the size of matrices with multiple ENPs present. However, the ability to quantitatively and rapidly detect the presence or absence of ENPs in the workplace would be an important step in providing a priori knowledge before more complex, expensive, and time-consuming investigatory tools (e.g., electron microscopy,

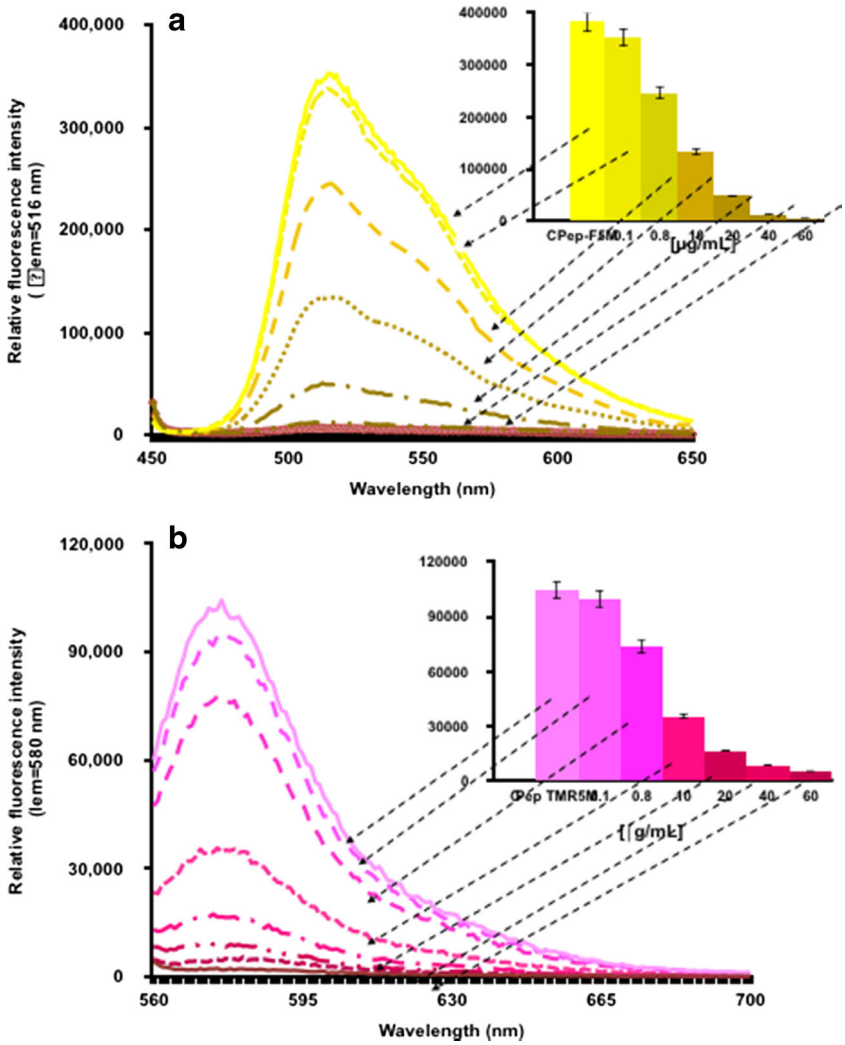


**Fig. 5** Concentration-dependent quenching of fluorescence of **a** fluorescein-5-maleimide-labeled peptide (*CPep-F5M*) and **b** tetramethylrhodamine-5-maleimide-labeled peptide (*CPep-TMR5M*) by gradual increase of the concentration of poly(acrylic acid)-capped $Fe_3O_4$ ENPs. The *y*-axis fluorescence intensity in arbitrary units (relative fluorescence units)

inductively coupled mass spectrometry, field-flow fractionation coupled with inductively coupled plasma mass spectrometry) are applied.

## Quenching of fluorescence by NOM solution was corrected with dilution

One of the potential drawbacks of a detection method that might involve environmental samples is interference from other compounds present in the water. Natural waters are complex, and one of the principal materials that are known to alter nanoparticle behavior in solution is NOM, primarily as humic acids [28]. Humic acids are released following decay of organic-plant-based materials, and the concentrations in the environment can range greatly from essentially zero in clear lakes to 50 mg/L in some environments [37]. Humic acid is known to rapidly interact with ENPs in solution, forming an "ecocorona" [38]. The presence of humic acid acts to stabilize ENPs in solution, resulting in reduced agglomeration, decreased average particle size, and increased stability in solution [37]. Importantly, for our studies, humic acid has the potential to interfere in at least three ways. First, humic acid displays autofluorescence when excited by light [36], and this may directly interfere with the assay readout. Second, given that NOM is able to absorb light of the wavelengths emitted by the fluorophores, it may serve as a quenching agent by absorbing the emitted light. Third, NOM may directly interfere (in a concentration-dependent manner) with the binding of the labeled peptide in the assay to the ENP because of the formation of the ecocorona and the displacement/shielding of potential binding sites. We tested these three hypotheses, and the results are presented in Fig. 6.

The presence of humic acid (10 μg/mL) and nanoparticles (10 μg/mL) in the reaction vessel (without peptide) did not result in substantial fluorescence (Fig. 6a). This clearly demonstrates that autofluorescence of the nanoparticles or humic acid was not a significant issue for our observing the fluorescence intensity. When F5M-labeled peptide was added to a mixture of nanoparticles and humic acid, there was an approximately 25 % reduction in fluorescence intensity,

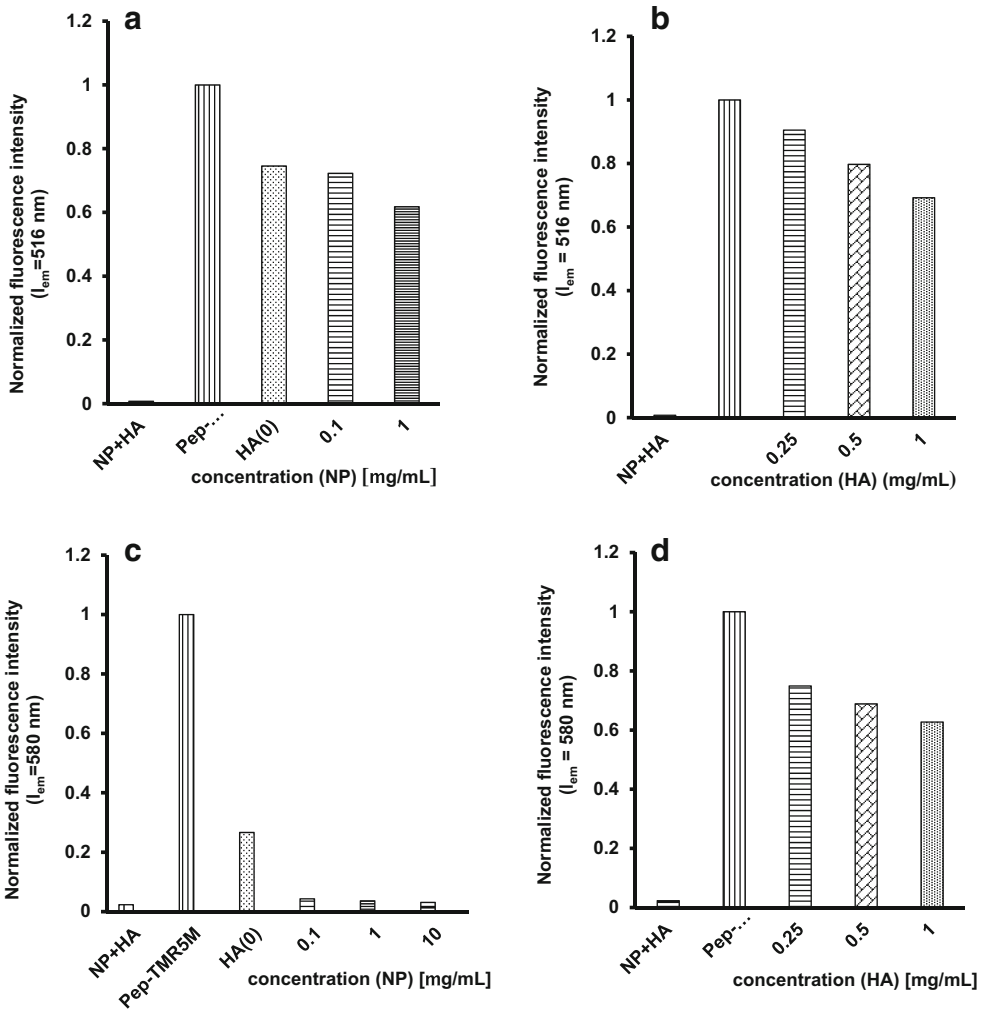


**Fig. 6** Interference of biosensor and ENP reaction corrected with dilution. **a** The reaction of nanoparticles and fluorescein-5-maleimide-labeled peptide (*Pep-5FM*) in organic medium [humic acid (*HA*) solution] has a reduced fluorescence quenching effect. **b** The reaction of nanoparticles and tetramethylrhodamine-5-maleimide-labeled peptide (*Pep-TMR5M*) significantly quenched the fluorescence signal. **c** The quenching effect in **a** was removed by reduction of the HA concentration. The quenching effect in **b** was reduced by reduction of the HA concentration. *NP* nanoparticles.

demonstrating some interference with the emission of the dye. This quenching of the signal may be due to absorption of either the excitation light or the emitted light as we cannot distinguish either scenario. However, as we increased the concentration of nanoparticles from 0.1 to 10 μg/mL, there was still a dose-dependent decrease in fluorescence intensity, demonstrating that the F5M-labeled peptides still function for detection in the presence of humic acid at a concentration up to 10 μg/mL (Fig. 6a). When we performed the same experiment using the TMR5M-labeled peptides, we found that similarly to the F5M-labeled peptides, there was not a significant interference from autofluorescence at the different wavelengths, although a small signal was detectable in all cases. However, humic acid had a severe impact on the fluorescence intensity of the dye, where humic acid at 10 μg/mL in the reaction vessel resulted in a more than 75 % reduction in fluorescence intensity. The reason for the great effect is likely the longer-wavelength emission spectrum of TMR5M and consequently great absorption by the humic acid and quenching of the signal. When nanoparticles were added at a very low concentration (0.1 μg/mL), almost no signal was detectable above the background autofluorescence and no dose dependence of nanoparticle concentration could be detected (Fig. 6c). The results of these and earlier experiments mean that TMR5M is considered a better dye overall for use in detection in pristine waters low in humic acid or in laboratory solutions. However, given that humic acid interferes with TMR5M-labeled-peptide-based detections, under conditions where humic acid is present, assays would require F5M-labeled peptides to be used since they are less affected by humic acid interference.

To test the effect of humic acid concentration on the function of the assay, we next examined the effect of increasing concentrations of humic acid on assay performance. Using the optimal peptide concentrations (see earlier) and nanoparticles at 10 μg/mL, we measured the fluorescence intensity in the presence of increasing concentrations of humic acid. As the humic acid concentration increased, there was a dose-dependent decrease in fluorescence intensity, showing that humic acid interfered with the assay for both F5M and TMR5M (Fig. 6b, d). Nevertheless, assuming humic acid concentration is accounted for in the assay with appropriate controls, these results demonstrate that the assay

is robust enough to measure nanoparticle concentrations up to 1 μg/mL.

Another drawback of the assay is that despite detection in the range that environmental and occupational exposures might occur, the assay does not allow positive identification of the material itself. However, in theory, one should be able to secondarily couple any positive result of detection with the results of a material-composition-based detection method (e.g., field-flow fractionation coupled with inductively coupled plasma mass spectrometry [39]) to identify the materials.

We also think that this development is potentially a valuable tool in an occupational health setting where workers may be exposed to specific ENPs and in scientific research where detection of materials during experiments is often difficult because of the inability to rapidly and easily measure concentrations of known substances in the test solutions. Detection of background materials and the presence of increased amounts of nanoparticles in a rapid time frame would be a valuable early assessment tool. For example, in research, following the concentration of a material during an experimental protocol is challenging because of agglomeration and settling. This method would allow rapid (less than 1 min) detection of the available monodisperse materials in the water column and improve experimental monitoring and interpretation of experiments. Similarly, in an occupational health setting, the method lends itself to a "wipe test" whereby the presence of specific materials in the workplace could be rapidly and quantitatively monitored. Moreover, our peptide-based detection method can be tailored to specific materials, and this may provide even better protection for workers and improve research in environmental and occupational nanosafety. There are still challenges to the implementation of these labeled peptides, including the potential for other interfering compounds or interference from natural nanosized materials. Regardless, with proper controls and precision, this method has the potential to achieve the desired goal.

## Conclusion

We have reported the development of two novel fluorescently labeled peptides that can detect a broad variety of ENPs in a quantitative manner and in less than 1 min. Currently, there are no rapid, inexpensive methods to detect ENPs in solution, and the use of these designer fluorescently labeled peptides has the potential to improve both experimental interpretation and occupational health and safety of workers.

**Acknowledgments** This study was supported by research funding to G.G.G. from both an Alberta Innovate Technology Futures nanoWorks grant (AITF no. NV 14402-2010; UA RES0004101) and an Natural Sciences and Engineering Research Council of Canada Strategic Project Grant (463674-14) with cosponsor support from Environment Canada and the National Institute of Nanotechnology.

**Compliance with ethical standards** No data, text, or theories by others is presented herein.

**Conflict of interest** The authors declare hat they have no conflict of interest.

## References

1. De Jong WH, Borm PJ. Drug delivery and nanoparticles: applications and hazards. Int J Nanomedicine. 2008;3:133–49.
2. Lee J, Mahendra S, Alvarez PJJ. Nanomaterials in the construction industry: a review of their applications and environmental health and safety considerations. ACS Nano. 2010;4:3580–90.
3. Qu X, Brame J, Li Q, Alvarez PJ. Nanotechnology for a safe and sustainable water supply: enabling integrated water treatment and reuse. Acc Chem Res. 2013;46(3):834–43.
4. Benn T, Cavanagh B, Hristovski K, Posner JD, Westerhoff P. The release of nanosilver from consumer products used in the home. J Environ Qual. 2010;39:1875–82.
5. Boczkowski J, Hoet P. What's new in nanotoxicology? Implications for public health from a brief review of the 2008 literature. Nanotoxicology. 2010;4:1–14.
6. Johnston HJ, Hutchison GR, Christensen FM, Peters S, Hankin S, Aschberger K, et al. A critical review of the biological mechanisms underlying the in vivo and in vitro toxicity of carbon nanotubes: the contribution of physico-chemical characteristics. Nanotoxicology. 2010;4:207–46.
7. Fabrega J, Luoma SN, Tyler CR, Galloway TS, Lead JR. Silver nanoparticles: behaviour and effects in the aquatic environment. Environ Int. 2011;37:517–31.
8. Zuo G, Kang S-G, Xiu P, Zhao Y, Zhou R. Interactions between proteins and carbon-based nanoparticles: exploring the origin of nanotoxicity at the molecular level. Small. 2013;9:1546–56.
9. Veerapandian M, Seo Y, Shin H, Yun K, Lee M. Functionalized graphene oxide for clinical glucose biosensing in urine and serum samples. Int J Nanomedicine. 2012;7:6123–36.
10. Newman JD, Setford SJ. Enzymatic biosensors. Mol Biotechnol. 2006;32:249–68.
11. Ronkainen NJ, Halsall HB, Heineman WR. Electrochemical biosensors. Chem Soc Rev. 2010;39:1747–63.
12. Wu J, Park JP, Dooley K, Cropek DM, West AC, et al. Rapid development of new protein biosensors utilizing peptides obtained via phage display. PLoS One. 2011;6(10), e24948.
13. Arya SK, Saha S, Ramirez-Vick JE, Gupta V, Bhansali S, Singh SP. Recent advances in ZnO nanostructures and thin films for biosensor applications: review. Anal Chim Acta. 2012;737:1–21.
14. Iqbal SS, Mayo MW, Bruno JG, Bronk BV, Batt CA, et al. A review of molecular recognition technologies for detection of biological threat agents. Biosens Bioelectron. 2000;15:549–78.
15. Luong JHT, Male KB. Glennon JD Biosensor technology: technology push versus market pull. Biotechnol Adv. 2008;26:492–500.
16. Dover JE, Hwang GM, Mullen EH, Prorok BC, Suh SJ. Recent advances in peptide probe-based biosensors for detection of infectious agents. J Microbiol Methods. 2008;78:10–9.

17. Vives E, Lebleu B. One-point labeling and purification of peptides and proteins with fluorescein maleimide. Tetrahedron Lett. 2003;44:5389–91.
18. Miyawaki A. Proteins on the move: insights gained from fluorescent protein technologies. Nat Rev Mol Cell Biol. 2011;12:656–68.
19. Wu B, Piatkevich KD, Lionnet T, Singer RH, Verkhusha VV. Modern fluorescent proteins and imaging technologies to study gene expression, nuclear localization, and dynamics. Curr Opin Cell Biol. 2011;23:310–7.
20. Kobayashi H, Choyke PL. Target-cancer-cell-specific activatable fluorescence imaging probes: rational design and in vivo applications. Acc Chem Res. 2011;44:83–90.
21. Felix LC, Ortega VA, Ede JD, Goss GG. Physicochemical characteristics of polymer-coated metal-oxide nanoparticles and their toxicological effects on zebrafish (Danio rerio) development. Environ Sci Technol. 2013;47(12):6589–96.
22. Felix L, Martinez-Rubi Y, Simard B, Goss G. Effects of functionalized singlewalled carbon nanotubes (SWCNTs) on embryonic zebrafish (Danio rerio). In: Nanotech Conference & Expo 2012. Technical proceedings, vol 3. Bio sensors, instruments, medical, environment and energy. Boca Ratio: CRC; 2012. p 327–30. http://www.nsti.org/procs/Nanotech2012v3/5/
23. Ong KJ, Zhao X, Thistle ME, MacCormack TJ, Clark RJ, Ma G, et al. Mechanistic insights into the effect of nanoparticles on zebrafish hatch. Nanotoxicology. 2014;8(3):295–304.
24. Bhomkar P, Goss GG, Wishart DS. A Simple and sensitive biosensor for rapid detection of nanoparticles in water. J Nanopart Res. 2014;16:2253–9.
25. Maccormack TJ, Clark RJ, Dang MK, Ma G, Kelly JA, Veinot JG, et al. Inhibition of enzyme activity by nanomaterials: potential mechanisms and implications for nanotoxicity testing. Nanotoxicology. 2012;6:514–25.
26. Stueker O, Ortega VA, Goss GG, Stepanova M. Understanding interactions of functionalized nanoparticles with proteins: a case study on lactate dehydrogenase. Small. 2014;10:2006–21.
27. Ong KJ, MacCormack TJ, Clark RJ, Ede JD, Ortega VA, Felix LC, et al. Widespread nanoparticle-assay interference: implications for nanotoxicity testing. PLoS One. 2014;9(3), e90650.
28. Hong SK, Elimelech MJ. Chemical and physical aspects of natural organic matter (NOM) fouling of nanofiltration membranes. J Membr Sci. 1997;132:159–81.
29. Kim JA, Salvati A, Aberg C, Dawson KA. Suppression of nanoparticle cytotoxicity approaching in vivo serum concentrations: limitations of in vitro testing for nanosafety. Nanoscale. 2014;6:14180–4.
30. Christenson HK. DLVO (Derjaguin–Landau–Verwey–Overbeek) theory and solvation forces between mica surfaces in polar and hydrogen-bonding liquids. J Chem Soc Faraday Trans 1. 1984;80:1933–46.
31. Wu RH, Nguyen TP, Marquart GW, Miesen TJ, Mau T, Mackiewicz MR. A facile route to tailoring peptide-stabilized gold nanoparticles using glutathione as a synthon. Molecules. 2014;19:6754–75.
32. Grillo R, Rosa AH, Fraceto LF. Engineered nanoparticles and organic matter: a review of the state-of-the-art. Chemosphere. 2015;119:608–19.
33. Vaccaro M, Mangiapia G, Radulescu A, Schillen K, D'Errico G, Morelli G, et al. Colloidal particles composed of amphiphilic molecules binding gadolinium complexes and peptides as tumor-specific contrast agents in MRI: physico–chemical characterization. Soft Matter. 2009;5:2504–12.
34. Tsai H, Lee A, Peng W, Yates MZ. Synthesis of poly(N-isopropylacrylamide) particles for metal affinity binding of peptides. Colloids Surf B: Biointerfaces. 2014;114:104–10. doi:10.1016/j.colsurfb.2013.09.060.
35. Zaman M, Ahmad E, Qadeer A, Rabbani G, Khan RH. Nanoparticles in relation to peptide and protein aggregation. Int J Nanomedicine. 2014;9:899–912.
36. Hawe A, Sutter M, Jiskoot W. Extrinsic fluorescent dyes as tools for protein characterization. Pharm Res. 2008;25(7):1487–99.
37. von der Kammer F, Ferguson PL, Holden PA, Masion A, Rogers KR, Klaine SJ, et al. Analysis of engineered nanomaterials in complex matrices (environment and biota): general considerations and conceptual case studies. Environ Toxicol Chem. 2012;31:32–49.
38. Chem KL, Elimelech M. Influence of humic acid on the aggregation kinetics of fullerene (C60) nanoparticles in monovalent and divalent electrolyte solutions. J Colloid Interface Sci. 2015;309:126–34.
39. Pace HE, Rogers NJ, Jarolimek C, Coleman VA, Gray EP, Higgins CP, et al. Single particle inductively coupled plasma-mass spectrometry: a performance evaluation and method comparison in the determination of nanoparticle size. Environ Sci Technol. 2012;46:1272–80.

**Oluyemi Akinloye** is Head of the Department of Medical Laboratory Science, Faculty of Basic Medical Science, College of Medicine of the University of Lagos, and he is Principal Investigator of the Reproductive, Oncology and Molecular Endocrinology Research Group. He is developing an African-based global consortium for scientific work on comparative genomics of prostate cancer. His research on genotoxicity of heavy metals and environmental toxicants was recently followed by rigorous work on nanotoxicology. He is a fellow of the Alexander von Humboldt Foundation and the Royal Society of Chemistry, an alumnus of the Marine Biology Research Laboratory and Harvard School of Public Heath, and a distinguished professor of clinical chemistry and laboratory medicine.

**Ramanarayan (Ram) Krishnamurthy** was a Research Associate at The Metabolomics Innovation Centre, University of Alberta, involved with analytical method development for the detection and characterization of metabolites and also an actively contributing member of the nanotechnology initiative entitled "New Technologies and Strategies for Assessment of Manufactured Nanomaterial Toxicity" at the University of Alberta with emphasis on development of peptide-based biosensors for the detection of nanoparticles. He is presently working as a supervisor at Maxxam Analytics Petroleum Technology Centre in Edmonton, Alberta, Canada.

**David Wishart** is a professor in the Departments of Biological Sciences and Computing Science at the University of Alberta. He is also a Senior Research Officer and the Program Coordinator for the Metabolomic Sensors Program at the National Research Council's National Institute for Nanotechnology. His research interests span many areas, including metabolomics, bioinformatics, structural biology, and nanotechnology.

**Greg Goss** is a Professor in biological sciences at the School of Public Health at the University of Alberta. He is a Fellow of the National Institute of Nanotechnology. His interdisciplinary research focuses on environmental testing and development of safer technologies and improved environmental sustainability for nanoscience. He serves on editorial boards for *Nanotoxicology* and *Environmental Science: Nano*. He is working directly with Environment Canada and the OECD on devising appropriate guidelines for testing of nanomaterials.